JOURNAL OF VIROLOGY, Sept. 2007, p. 9050–9060 Vol. 81, No. 17
0022-538X/07/$08.00+0 doi:10.1128/JVI.00479-07

Hepatitis B Virus Maturation Is Sensitive to Functional Inhibition of ESCRT-III, Vps4, and γ2-Adaptin▽

Carsten Lambert, Tatjana Döring, and Reinhild Prange*

Department of Medical Microbiology and Hygiene, Johannes Gutenberg-Universität Mainz, D-55101 Mainz, Germany

Received 7 March 2007/Accepted 1 June 2007

Hepatitis B virus (HBV) is an enveloped DNA virus that presumably buds at intracellular membranes of infected cells. HBV budding involves two endocytic host proteins, the ubiquitin-interacting adaptor γ2-adaptin and the Nedd4 ubiquitin ligase. Here, we demonstrate that HBV release also requires the cellular machinery that generates internal vesicles of multivesicular bodies (MVBs). In order to perturb the MVB machinery in HBV-replicating liver cells, we used ectopic expression of dominant-negative mutants of different MVB components, like the ESCRT-III complex-forming CHMP proteins and the Vps4 ATPases. Upon coexpression of mutated CHMP3, CHMP4B, or CHMP4C forms, as well as of ATPase-defective Vps4A or Vps4B mutants, HBV assembly and egress were potently blocked. Each of the MVB inhibitors arrested virus particle maturation by entrapping the viral core and large and small envelope proteins in detergent-insoluble membrane structures that closely resembled aberrant endosomal class E compartments. In contrast, HBV subvirus particle release was not affected by MVB inhibitors, hinting at different export routes used by viral and subviral particles. To further define the role γ2-adaptin plays in HBV formation, we examined the effects of its overexpression in virus-replicating cells. Intriguingly, excess γ2-adaptin blocked HBV production in a manner similar to the actions of CHMP and Vps4 mutants. Moreover, overexpressed γ2-adaptin perturbed the endosomal morphology and diminished the budding of a retroviral Gag protein, implying that it may act as a principal inhibitor of the MVB sorting pathway. Together, these results demonstrate that HBV exploits the MVB machinery with the aid of γ2-adaptin.

In order to be released from cells, nonlytic enveloped viruses must undergo budding from either the plasma membrane or intracellular membranes, followed by pinching off or fission. The fission event is facilitated by virus-encoded late assembly domains that recruit and hijack the cellular budding machinery of multivesicular bodies (MVBs) (3, 31). In the cell, MVBs have the unique ability to generate intraluminal vesicles that bud away from the cytosol, a process topologically equivalent to that of enveloped virus budding. Sorting of cellular proteins toward internal MVB vesicles for either degradation, lysosomal functions, or exosomal release requires the coordinated actions of at least three hetero-oligomeric complexes, referred to as ESCRT (endosomal sorting complex required for transport) complexes I, II, and III (ESCRT-I, -II, and -III) (1, 2, 20, 35, 40). They are sequentially recruited to the late endosomal membrane and drive the formation of MVBs. After sorting, the process is terminated by the AAA-type ATPase Vps4, which disassembles and thereby recycles the ESCRT machinery. The functional loss of individual subunits of this machinery results in a malformed, dysfunctional MVB known as the "class E compartment" (4, 9, 11).

In recent years, intense research has begun to uncover how enveloped RNA viruses utilize components of the MVB sorting pathway for the formation of progeny particles that mostly bud at the plasma membranes of infected cells (3, 30, 31, 41, 43). By contrast, mechanisms and sites of particle budding in families of enveloped DNA viruses, like the hepadnavirus family, are less defined. Hepatitis B virus (HBV) is the prototype member of this virus family, comprising small viruses that have extremely limited coding capacities and presumably therefore must recruit and reprogram cellular proteins to assist in the budding process (6, 10). HBV assembly begins with the formation of icosahedral nucleocapsids that package the viral pregenomic RNA, together with the viral polymerase. Inside the capsids, formed by 120 dimers of the single core protein, the partially double-stranded 3.2-kb DNA genome is synthesized through reverse transcription of the pregenomic RNA (32). Mature nucleocapsids, formed in the cytoplasm, can then be enclosed by the viral envelope composed of cellular lipids and three viral glycoproteins, the small (S), middle (M), and large (L) envelope proteins, that originate at the endoplasmic reticulum (ER) membrane (6, 16). Capsid envelopment strictly depends on the L protein, while S is required but not sufficient, and M is dispensable (6). However, it is poorly understood where in the host cell HBV capsids recruit the envelope during budding. Because the HBV envelope proteins do not appear in the plasma membrane (12) and because solitary expression of the S envelope protein leads to the assembly of empty subviral envelope particles that bud at post-ER/pre-medial-Golgi membranes and leave the cell via the classic constitutive pathway of secretion (17, 33), the canonical view is that the budding of subviral S envelope particles reflects the budding of virions.

However, previous analyses implied that HBV virus trafficking and budding involve endosomal compartments and at least two presumptive endosomal proteins, namely, γ2-adaptin and Nedd4. These act at the late stages of virus assembly, likely in conjunction with ubiquitin (15, 21, 37). γ2-Adaptin is highly similar to γ1-adaptin, one large subunit of the *trans*-Golgi

* Corresponding author. Mailing address: Department of Medical Microbiology and Hygiene, University of Mainz, Augustusplatz, D-55101 Mainz, Germany. Phone: 49-6131-3936750. Fax: 49-6131-3932359. E-mail: prange@mail.uni-mainz.de.

▽ Published ahead of print on 6 June 2007.

network/endosome adaptor protein (AP) complex AP-1, but nonetheless serves a separate, still unknown function (25, 42, 45). For HBV, γ2-adaptin proved to be one key budding factor, as it establishes productive interactions with both the viral envelope and the capsid, possibly to link the viral substructures at the budding site (15, 37). The reduction of the γ2-adaptin level by siRNA treatment blocks HBV assembly and egress, notably without compromising subviral S envelope particle release (37). Another clue for a linkage of the HBV budding strategy to endosomal/MVB sorting pathways is based on our finding that the cellular Nedd4 ubiquitin ligase controls virus production by binding to the late assembly domain-like PPAY motif of HBV capsids (37). Nedd4 family members per se are not part of the MVB machinery but help to sort ubiquitinated cargo proteins into MVB vesicles and are coopted by several enveloped RNA viruses to gain access to the inner MVB budding apparatus (3, 18, 29).

At least two important questions are raised by these findings. First, does HBV access the MVB machinery to bud from cells? Second, how does γ2-adaptin, a ubiquitin receptor presumably acting in the endocytic pathway, assist in virus budding? To address these issues, we analyzed HBV maturation in virus-replicating liver cell lines in which ESCRT-III, Vps4, and γ2-adaptin functions had been inactivated. We provide evidence that HBV is yet another example of an enveloped virus and the first example of a DNA virus, exploiting the endosomal sorting pathway with the aid of γ2-adaptin.

MATERIALS AND METHODS

DNA constructs. For HBV replication in permissive liver cell lines, plasmid pHBV was used. It carries an 1.1-mer of the HBV DNA genome in which the viral core/polymerase promoter is preceded by the human metallothionein IIa promoter, while the envelope open reading frame is under the transcriptional control of its authentic promoters (36). Plasmid pHBV.C$^-$ is identical to pHBV with the exception that a stop codon was created at triplet 38 of the core gene to ablate core expression and, hence, HBV replication (36). For solitary expression of the HBV core or S envelope gene, plasmids pNI2.C and pNI2.S, respectively, were employed (37). The expression vector pcDNA3-HA-γ2 containing the human γ2-adaptin cDNA with an N-terminal hemagglutinin (HA) tag (42) was a gift from K. Nakayama (Tsukuba University, Japan). The expression vectors encoding human wild-type (wt) and mutant Vps4A and Vps4B proteins (11) were generously provided by W. Sundquist (University of Utah). In brief, wt Vps4A or its E228Q point mutant was fused in frame to the C terminus of green fluorescent protein (GFP), while Vps4B and its E235Q variant were expressed as C-terminal fusions of a red-shifted GFP version (DsRed). The mammalian expression vectors pCHMP3.YFP, pCHMP4B.DsRed, and pCHMP4C.GFP encoding dominant-negative (dn) forms of human charged MVB proteins (CHMPs) were kindly provided by E. Gottwein (University of Heidelberg, Germany). As negative controls, the corresponding empty pEYFP, pDsRed, and pEGFP plasmids were used. The expression vector of murine leukemia virus (MLV) Gag full-length precursor protein, in which the viral polymerase was replaced by yellow fluorescent protein (YFP) (39), was generously provided by W. Mothes (Yale University Medical School) via Addgene as "Addgene plasmid 1813."

Antibodies. For immunoprecipitation of HBV particles, a mixture of rabbit antibodies against the L and S envelope proteins was used as described previously (27). To detect L by Western blotting, the mouse monoclonal MA18/7 antibody (16) was used (a gift from K.-H. Heermann, University of Göttingen, Germany). The S-specific immunoblotting was done with rabbit R247 anti-S antibodies (19) (a gift from C. Sureau, Laboratoire de Virologie Moléculaire, France) or goat 70-HG15 anti-S antibodies (Fitzgerald Industries International). Polyclonal antisera against recombinant native or denatured core particles were raised in rabbits as described previously (37). Commercially available antibodies were as follows: mouse antibodies against the HA epitope tag (BabCO), anti-HA rat antibodies (Roche Applied Science), anti-GFP mouse antibodies (BD Biosciences), mouse antibodies against human heat shock protein Hsc70 (StressGen Biotechnologies), mouse antibodies against human CD63 (Santa Cruz), mouse antibodies specific for human protein disulfide isomerase (PDI) (StressGen Biotechnologies), and rabbit antiserum against the human *cis*/medial 58K Golgi marker (Sigma). The antibodies recognizing human Rab2, Rab5, and Rab7 were purchased from Santa Cruz. Peroxidase-labeled secondary antibodies were obtained from Dianova, and fluorophore-labeled antibodies were purchased from Molecular Probes. All antibodies were applied in dilutions recommended by the suppliers.

Cell culture, transfection, and lysis. The human hepatocellular carcinoma cell line HuH-7 was used throughout. Transfections with plasmid DNAs were performed with Lipofectamine Plus (Invitrogen) according to the manufacturers' instructions. The amounts of plasmid DNA used in (co)transfection experiments are indicated in the corresponding figure legends and in Results. Unless otherwise indicated, cells were lysed 3 days after transfection.

To probe for protein expression and protein solubility, transfected cells were lysed with either the nondenaturing detergent Nonidet P-40 (NP-40) or the denaturing reagent sodium dodecyl sulfate (SDS). NP-40 lysates were prepared by incubating the cells with Tris-buffered saline (50 mM Tris-HCl, pH 7.5, 150 mM NaCl) containing 0.5% NP-40 for 20 min on ice. Thereafter, the lysates were centrifuged for 5 min at 15,000 × *g* and 4°C. For cell lysis with SDS, the cells were scraped from the plates using 1× Laemmli buffer, and the cell suspensions were boiled for 10 min prior to centrifugation. Cell extracts were subjected to SDS-polyacrylamide gel electrophoresis and Western blotting analyses using standard procedures.

Detection of released particles. To monitor the assembly and secretion of HBV subviral envelope particles, NP-40 lysates and clarified cell culture media of transfected cells were analyzed by an S-specific enzyme-linked immunosorbent assay (ELISA) (Auszyme; Abbott). To analyze the release of virus-like capsid particles (VLPs) from MLV Gag-transfected cells, culture medium was filtered on 0.45-μm membranes and concentrated by ultracentrifugation through a 20% sucrose cushion (4 h at 100,000 × *g* and 4°C). After being washed in Tris-buffered saline, the pellets were suspended in 1× Laemmli buffer.

Subcellular fractionation. Endosomal fractions were prepared and separated from microsomal fractions by flotation gradient analysis according to a protocol described by Kobayashi et al. (22). Briefly, transfected cells were homogenized and a postnuclear supernatant was prepared. The postnuclear supernatant was adjusted to 40.6% sucrose, 3 mM imidazole, pH 7.4; loaded at the bottom of an SW60 tube; and overlaid sequentially with 35, 25, and 7.5% sucrose solutions in 3 mM imidazole, pH 7.4. After centrifugation of the gradient for 1 h at 100,000 × *g*, 10 fractions were collected from the top, and the proteins of each fraction were precipitated with trichloroacetic acid prior to immunoblot analyses.

Detection of intracellular HBV nucleocapsids, extracellular virions, and viral DNA. For HBV replication in HuH-7 cells, the replicon plasmid pHBV was used. After transfection, cellular supernatants were harvested, and cell lysates were prepared with the nondenaturing detergent Triton X-100. Intracellular nucleocapsids and extracellular virions were isolated by capsid- or envelope-specific immunoprecipitations, respectively, prior to detection of the encapsidated viral progeny DNA by radioactive labeling of the partially double-stranded genome with [α^{32}P]dCTP (GE Healthcare Biosciences) by the endogenous polymerase as described previously (27). After extraction of the labeled DNA genomes from the immunoprecipitated samples, they were resolved by agarose gel electrophoresis and visualized by phosphorimaging (GE Healthcare Biosciences).

Alternatively, the viral progeny DNA was detected by Southern blotting. Five days after transfection, cells were lysed in the culture dish by adding 1 ml of DNA lysis buffer (10 mM Tris-HCl, pH 8.0, 25 mM EDTA, 1% SDS). Samples were then digested with RNase A (20 μg/ml) for 1 h at 37°C, followed by overnight incubation with proteinase K (100 μg/ml) at 50°C. To purify total DNA, samples were subjected to phenol-chloroform extraction until they were clean, and DNA was precipitated with ethanol. Twenty micrograms of total DNA was denatured by boiling it in 0.4 M NaOH, 10 mM EDTA and filtered with a dot blot manifold (Schleicher & Schüll) onto nylon membranes. The membranes were baked at 120°C for 30 min and hybridized with an EcoRI-linearized unit-length HBV genome that was labeled with digoxigenin-dUTP by random priming as instructed by the manufacturer (Roche). Hybridization and detection were performed according to the Roche DIG DNA labeling and detection kit.

Immunofluorescence. For immunofluorescence microscopy, cells grown on coverslips were fixed 2 days posttransfection and permeabilized with ice-cold methanol containing 2 mM EGTA for 2 to 10 min at −20°C. After being washed and blocked for 30 min in phosphate-buffered saline containing 2% normal serum, the cells were incubated with primary antibodies for 1 h at 37°C, rinsed with phosphate-buffered saline, and then incubated with AlexaFluor-tagged secondary antibodies for 1 h at 37°C. The nuclear stain was added in the last 10 min. Following washing and mounting of the cells, microscopic analysis was per-

formed with an Axiovert 200 M fluorescence microscope (Zeiss) using a 100× (numerical aperture, 1.25) oil immersion objective. AxioVision (Zeiss) and Adobe Photoshop CS were used for processing of the images.

RESULTS

HBV envelope and core proteins are detectable in endosomal compartments. We previously observed by immunofluorescence studies of HBV-replicating cells that a subset of the viral core particles and the large L envelope protein colocalize in compartments positive for CD63, a tetraspanin found in late endosomes and MVBs (37). To further substantiate this finding, we applied a biochemical fractionation approach. Therefore, human hepatoma HuH-7 cells were transiently transfected with an expression vector carrying a replication-competent HBV genome (HBV replicon). Of note, transfected liver cell lines support the production of infectious virions but are refractory to the uptake of progeny HBV particles (12). After transient transfection, endosomal fractions were prepared and separated from microsomal fractions by a flotation gradient analysis. The assignments of microsomal compartments, like the ER, intermediate compartment (IC), and Golgi fractions, were based on the marker analyses using anti-PDI, anti-Rab2, and anti-58K antisera, respectively. To probe for the distribution of endosomal compartments, the gradient was assayed for the endosomal markers Rab5 and Rab7. As shown in Fig. 1, endosomes were found to be enriched in lighter fractions with a peak in fraction 4, while the secretory compartments exclusively banded in the denser fractions. Given the sufficient separation of endosomes from the microsomal compartments, fractions were next assayed for the distribution of the HBV L and S envelope proteins. Consistent with previous results (23), the nonglycosylated p39 and glycosylated gp42 forms of L, as well as the nonglycosylated p24 and glycosylated gp27 forms of S, were present in the ER, IC, and *cis*/medial Golgi fractions (Fig. 1). Importantly, L and S were also found in the lighter fractions comprising endosomal compartments (Fig. 1). Similar results were obtained when the gradient was probed for the distribution of the core protein. As is the case for L and S, a significant portion of core was found to coincide with the Rab5- and Rab7-positive endosomal fraction 4 (Fig. 1). These data, together with our previous results (37), indicate that HBV appears to utilize endosomal membranes as assembly sites and/or to traverse through endosomes during exit from the hepatocyte.

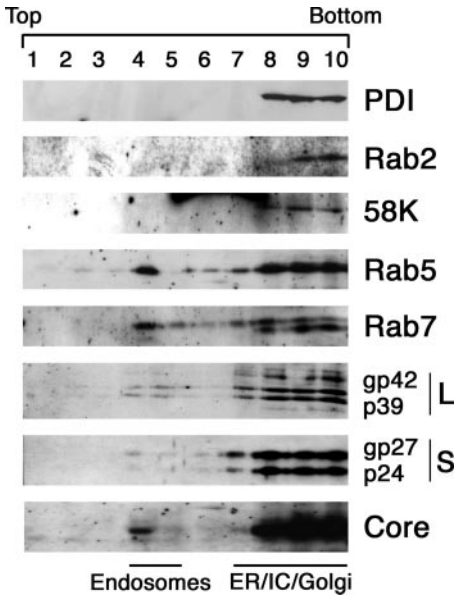

FIG. 1. HBV envelope and core proteins are detectable in endosomal compartments. For preparation of endosomes, HBV-replicating HuH-7 cells were homogenized and fractionated by flotation in a sucrose gradient using a well-established protocol (22). After 10 fractions, designated 1 to 10, were collected, they were probed for the assignment of marker for the ER (PDI), the IC (Rab2), the Golgi complex (58K), and endosomes (Rab5 and Rab7) by specific immunoblotting. The same fractions were assayed for the distribution of the HBV L and S envelope proteins and the core protein by using the MA18/7 antibody, the R247 antibody, and anti-core antiserum, respectively. At the bottom of the blot, the deduced gradient positions of endosomes and secretory compartments are indicated. Quantitation of the signals revealed that 20% of total microsomal Rab5, 27% of Rab7, 11% of L, 9% of S, and 18% of core were present in the corresponding endosomal fractions.

Dn CHMP and Vps4 mutants block HBV particle assembly and release without affecting virus genome replication. Several works have established that components of the cellular MVB pathway that normally sort ubiquitinated cargo toward internal vesicles also play a direct role in the budding and release of many enveloped RNA viruses (3, 31, 35, 40). Given the association of HBV with endosomal structures, we sought to analyze whether it may also exploit MVB pathway functions for particle assembly and egress. The MVB apparatus can be biochemically separated into ESCRT-I (20), -II (2), and -III (1) complexes accompanied by accessory proteins that perform a coordinated cascade of events, so that ESCRT-I and -II mediate the recognition and sorting of ubiquitinated cargo and then initiate the recruitment of ESCRT-III to the membrane (43, 44). ESCRT-III appears to be the core of the machinery and is composed of the CHMPs, responsible for the budding and membrane fission events during vesicle formation (1). Finally, ESCRT-III recruits the ATPase Vps4, which disassembles and releases the complexes upon ATP hydrolysis (4, 9). To perturb the ESCRT network in HBV-replicating cells, we used two strategies. First, for interference with ESCRT-III functions, we used ectopic expression of dn forms of a subset of CHMP proteins, like CHMP3, a proven subunit of ESCRT-III, as well as CHMP4B and CHMP4C, two putative components of the complex (24, 30, 41, 43). CHMP proteins can be converted to potent dn forms by fusion to a large heterologous protein, like GFP or its derivatives (30, 41, 43). As a second approach to impair the MVB pathway, we employed ATP hydrolysis-deficient mutants of Vps4. The two mammalian Vps4 isoforms, Vps4A and Vps4B, can be potently blocked by overexpression of their corresponding mutants that lack the ATPase activity and act in a *trans*-dn manner (4, 9, 11, 26).

To analyze whether an intact ESCRT-III complex and functional Vps4 are required for HBV production, HuH-7 cells were cotransfected with the HBV replicon and expression vectors for wt and mutant forms of CHMP and Vps4. To interfere with CHMP functions, the three dn fusion constructs CHMP3-YFP, DsRed-CHMP4B, and cyan fluorescent protein-CHMP4C were individually coexpressed, whereas Vps4 activity was ablated by coexpression of the GFP-tagged Vps4A and DsRed-tagged

Vps4B mutants with defects in ATP hydrolysis (E228Q and E235Q, respectively). For simplification, all five dn mutants are denoted by their names with the suffix "dn" in the figures, whereas the wt proteins are marked with "wt." Because overexpression of such dn constructs has been reported to possibly cause cytotoxic effects (11, 41, 43), we first tested different DNA ratios in the cotransfection experiments. While the overall cell viability was indeed impaired at a 1:1 DNA ratio of the HBV replicon to the dn mutants, no effect was apparent when the dn mutant DNAs were lowered 5- to 10-fold. Under these conditions, all wt and dn constructs were efficiently synthesized, as evidenced by immunoblotting and fluorescence microscopy (see Fig. 3, 4, and 7). None of the constructs affected the amount of the cell-associated cognate heat shock protein Hsc70, which we used as a marker to monitor overall protein synthesis and cell viability (Fig. 2A). Next, HBV production and release were analyzed using immunoprecipitation of cellular supernatants with envelope-specific antisera, radioactive labeling of the partially double-stranded DNA genome by the viral endogenous polymerase, and detection of the genome by gel electrophoresis. In parallel, intracellular nucleocapsid assembly was investigated by the endogenous polymerase reaction (EPR) using core particle-specific antibodies for immunoprecipitation of lysates that were prepared with the nonionic detergent Triton X-100. As shown in Fig. 2A, dramatic effects were observed for the three dn CHMP3, CHMP4B, and CHMP4C constructs, which all reduced virus release to nearly undetectable levels, even at a DNA ratio as low as 1:10. Unexpectedly, however, the amounts of nucleocapsids detected inside the cell were also severely diminished by each CHMP fusion. The same results were obtained with HBV-replicating cells expressing dn versions of Vps4A and Vps4B (Fig. 2A). Although these cells proved to be as viable as cells transfected with the corresponding wt vectors, the presence of the ATPase-defective Vps4A and Vps4B mutants significantly interfered with both nucleocapsid assembly and virus export (Fig. 2A). Because all dn mutants reduced the amounts of nucleocapsid-associated intracellular progeny HBV DNA, it remained possible that they affected overall HBV replication. To analyze this possibility, total DNA was extracted from cells 5 days after transfection and subjected to HBV-specific Southern dot blotting (Fig. 2B). As a control, cells were transfected with a cloned HBV genome that was defective in replication due to an ablation of core gene expression (HBV.C$^-$). The dot blot analysis of HBV.C$^-$-transfected cells revealed a very weak signal, which likely reflected the hybridization of the labeled probe with residual transfected HBV plasmid DNA (Fig. 2B). In contrast, the signals obtained with total DNA isolated from HBV-(co)transfected cells were significantly stronger, indicating productive HBV genome replication. As demonstrated for CHMP4C- and Vps4A-expressing cells, none of the dn constructs reduced the amount of replicative HBV DNA (Fig. 2B) and hence affected the viral polymerase. Collectively, these data demonstrate that late stages of HBV maturation depend on the actions of CHMP and Vps4.

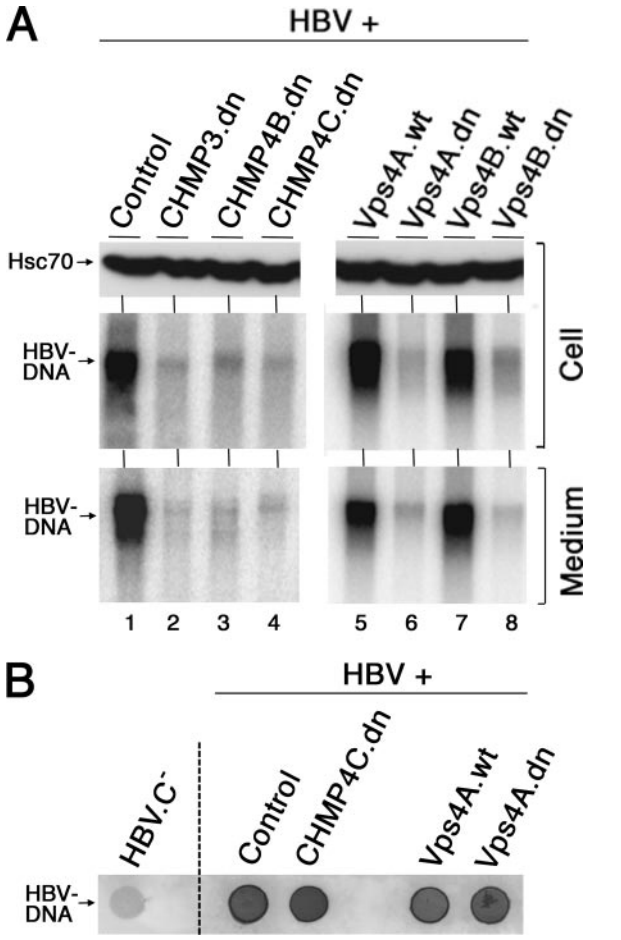

FIG. 2. Dn CHMP and Vps4 mutants block HBV particle assembly and release without affecting virus genome replication. (A) HuH-7 cells were cotransfected with the HBV replicon (HBV) and CHMP3-YFP (CHMP3.dn), DsRed-CHMP4B (CHMP4B.dn), or cyan fluorescent protein-CHMP4C (CHMP4C.dn) expression vectors or a GFP vector serving as a negative control at a 9:1 DNA weight ratio. For Vps4, GFP/DsRed-tagged wt and dn versions of Vps4A and Vps4B were cotransfected with HBV at a 1:9 DNA weight ratio, as indicated above each lane. Three days posttransfection, cellular supernatants (Medium) and cytoplasmic extracts (Cell) were harvested. Cells were assayed for overall protein expression and fitness by Western blot analysis of lysates with an anti-Hsc70 antibody (top). HBV release into the medium was detected by immunoprecipitation of total supernatants and radioactive labeling of the viral genome by the viral polymerase (EPR). The migration of the HBV genome, as visualized by agarose gel electrophoresis and phosphorimaging, is indicated (bottom). Nonenveloped cytoplasmic nucleocapsids were immunoprecipitated from cell lysates (50% of lysates) and processed by EPR (middle). (B) HuH-7 cells were cotransfected with the indicated constructs as described above and were lysed 5 days posttransfection. For a negative control, cells were individually transfected with a plasmid encoding a replication-defective HBV replicon (HBV.C−). Twenty micrograms of total cellular DNA isolated from lysed cells was processed by Southern dot blotting using a digoxigenin-dUTP-labeled HBV-specific probe.

Dn CHMP and Vps4 mutants trap HBV core, L, and S in detergent-insoluble membranes. The aforementioned results implied that HBV utilizes MVB pathway functions, but it remained unclear how the dn CHMP and Vps4 mutants arrested virus particle production. To address this question, we investigated the expression and distribution profiles of the viral key structural proteins, core and L, in HBV-replicating cells that were cotransfected essentially as outlined in Fig. 2. In addition, we also focused on the S envelope protein that forms the scaffold of the viral envelope but is itself defective in capsid envelopment (6). Cell extracts were prepared with the nonionic detergent NP-40 and assayed for the amounts of core, L,

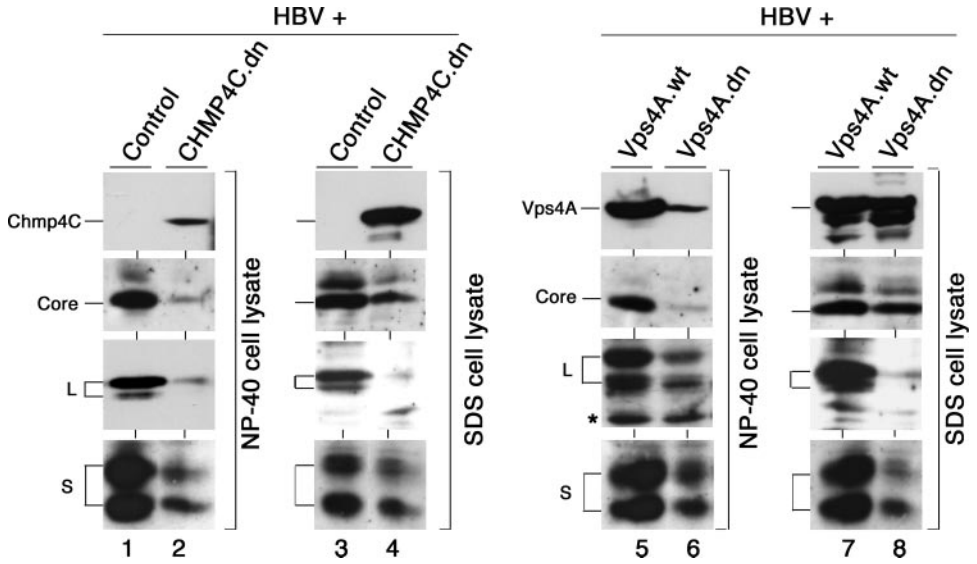

FIG. 3. Dn CHMP and Vps4 sequester HBV core, L, and S to detergent-insoluble membranes. HuH-7 cells were cotransfected in duplicate with the HBV replicon (HBV), together with CHMP4C.dn or its relevant control or together with the wt or dn Vps4A expression plasmids at 9:1 DNA weight ratios. Lysates were prepared using either NP-40 or SDS, and equal amounts of the lysates (25% of the lysates) were subjected to SDS-polyacrylamide gel electrophoresis and immunoblotting with an antibody against the GFP tag of the Vps4A and CHMP4C constructs (top), an anti-core antiserum (top middle), an anti-L antibody (bottom middle), and the anti-S 70-HG15 antibody (bottom). The migration of the corresponding proteins is indicated on the left. In the L-specific blot shown in lanes 5 and 6, the star marks a nonspecifically stained band that served as a control for identical gel loading.

and S by Western blot analysis. Intriguingly, the levels of all proteins were significantly lower when a dn form was present, as exemplified for CHMP4C- and Vps4A-expressing cells in Fig. 3 (lanes 1 and 2, 5 and 6). Because none of the dn constructs reduced the intracellular amount of Hsc70 (Fig. 2) or the synthesis of an ectopically coexpressed reporter protein (data not shown), the dn CHMP4C- and Vps4A-imposed reductions of core, L, and S were likely specific.

Many dominant inhibitors of the MVB pathway have been shown to function by inducing the formation of dysfunctional, aberrantly enlarged endosomes, referred to as class E compartments. On their surfaces, the inhibitors accumulate and sequester other MVB factors and cargoes into large detergent-insoluble complexes (4, 9, 26, 41). It therefore appeared possible that the decrease of cell-associated core, L, and S might be due to their entrapment on aberrant endosomes induced by dn CHMP4C and Vps4A. To address this point, cells were lysed in more stringent buffer in the presence of the denaturing reagent SDS. As shown in Fig. 3, both dn CHMP4C and Vps4A could be recovered in significantly larger quantities in the SDS lysates than in the NP-40 lysates, thus confirming their abilities to induce detergent-insoluble complexes to which they themselves were drawn. Importantly, almost equal core levels could be detected in the SDS lysates, irrespective of whether wt/controls or dn CHMP4C and Vps4A were coexpressed (Fig. 3). However, we failed to solubilize L even upon SDS extraction, which might be due to its firm transmembrane configuration (Fig. 3). For S, significant but not total amounts could be recovered in the SDS extracts. We conclude from these results that dn CHMP4C and Vps4A inhibited HBV formation by entrapping the viral subunits in NP-40-resistant structures. This in turn reduced the physiological intracellular accumulation of the viral subunits, with the consequence that less was available for budding and release.

Dn CHMP and Vps4 mutants trap HBV core and L in class E-like compartments. To determine if the change in extractability of core and L proteins reflected their association with aberrant endosomes, we performed immunofluorescence analysis of HBV/Vps4A-cotransfected cells. Consistent with several reports (4, 9, 26), GFP-tagged wt Vps4A exhibited diffuse staining throughout the cell, whereas dn Vps4A accumulated in clustered foci (Fig. 4). In the presence of wt Vps4A, the HBV core revealed its typical staining pattern and was distributed in both the cytoplasm and the nucleus at steady state (Fig. 4). In contrast, coexpression of dn Vps4A dramatically altered the distribution of core so that it exhibited a punctate pattern reminiscent of dn Vps4A-induced aberrant clusters of vacuoles. A redistribution induced by dn Vps4A was also observed for L, which revealed faint perinuclear ER-like and juxtanuclear Golgi-like staining in control cells (Fig. 4). Upon coexpression of dn Vps4A, L now accumulated in punctate dots that largely stained positive for dn Vps4A and resembled perturbed endosomal structures. Of note, L was readily detectable in Vps4A-inactivated cells by this experimental approach, indicating that its absence in lysates of correspondingly transfected cells (Fig. 3) was likely due to its insolubility. A similar sequestration of core and L on aberrant endosomal vacuoles was evident when the dn Vps4B isoform and the three dn CHMP3/4B/4C fusion constructs were analyzed by immunofluorescence microscopy (data not shown). To ask more directly whether the enlarged vacuoles induced by the dn inhibitors resembled endosomal structures, HBV-replicating cells coexpressing dn Vps4A were immunostained with antibodies against CD63, a marker for late endosomes and MVBs. As

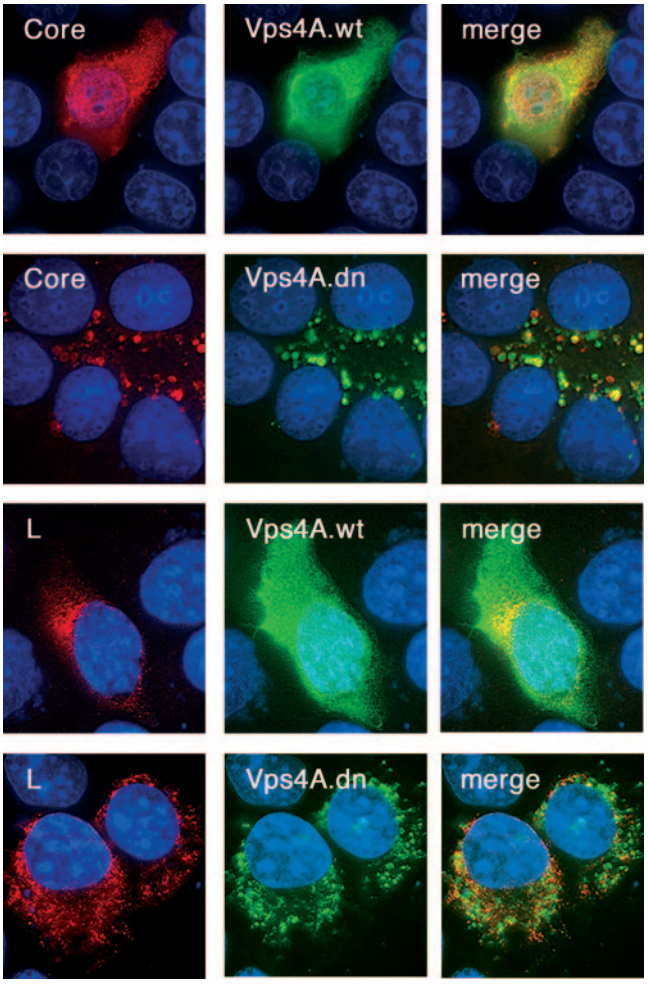

FIG. 4. Dn Vps4A redistributes HBV core and L to aberrant endosomal class E compartments. HuH-7 cells were cotransfected with the HBV replicon and GFP-tagged Vps4A.wt (rows 1 and 3 from top) or Vps4A.dn (rows 2 and 4 from top). Two days after transfection, the cells were fixed and immunostained for core (rows 1 and 2) and L (rows 3 and 4) using rabbit anti-core and mouse anti-L antibodies, respectively. The primary antibodies were followed by staining with AlexaFluor 564-conjugated goat anti-rabbit or anti-mouse immunoglobulin antibodies, and the fluorescent signals of core and L (red) are shown in the left columns. The GFP fluorescence of Vps4A was visualized directly (green) and is indicated in the middle column. The overlays of the fluorescences are shown in the right column, with yellow indicating colocalization. DNA staining of the cell nuclei is shown in blue.

shown in Fig. 5, most of these vacuoles had CD63 on their peripheries. When cells were costained with anti-L or anti-core antibodies, we observed substantial colocalization of both viral proteins with CD63 on the perturbed endosomal structures. Together, these results indicate that both groups of MVB inhibitors suppressed HBV production by similar mechanisms of action, i.e., by entrapping the viral core and L in vacuolated class E-like compartments.

Dn CHMP and Vps4 mutants do not block subviral S envelope particle assembly and release. HBV morphogenesis is accompanied by the formation of subviral envelope particles that lack the nucleocapsid. Subviral spherical particles are composed of the S and M proteins and contain only small amounts of the L protein, whereas the relative amount of L is higher in filamentous particles (6). Upon solitary expression of the S protein, subviral S envelope particles have been shown to mature by budding into intraluminal cisternae of post-ER/pre-Golgi compartments and to leave the cells via secretion (17, 33). To investigate whether the maturation of such S envelope particles also involves endosomal pathway functions, cells were cotransfected with an expression vector carrying only the HBV S gene, together with wt or dn versions of CHMP4C and Vps4A. Twenty-five percent of total cell lysates, made with the nonionic detergent NP-40, and 12.5% of cell supernatants were probed by an S-specific ELISA. This analysis revealed that neither dn CHMP4C nor dn Vps4A grossly impaired subviral S envelope particle assembly and release (Table 1). These results were surprising, since a substantial fraction of S was shifted to detergent-insoluble membranes upon HBV production in MVB-inhibited cells (Fig. 3). One likely interpretation of the different behaviors of S in cells expressing this protein alone and in the context of ongoing virus replication could be that L might take away a fraction of S, required for virus formation, to MVB pathway functions. To address this point, we analyzed the assembly and budding of subviral particles that contained L, as well as S. The cells were transfected with the replication-defective HBV.C$^-$ construct that carries the viral-envelope open reading frame under the control of its authentic promoters (Env). The S-specific immunoassay of NP-40 lysates (25%) and cell supernatants (12.5%) indeed revealed that both dn CHMP4C and dn Vps4A significantly diminished subviral envelope particle assembly and egress when S was coexpressed with L (Table 1). We conclude from these results that the formation and budding of subviral envelope particles composed of S alone do not require MVB pathway functions. Hence, the mechanisms of subviral S envelope particle and HBV particle production appear to differ in their requirements for cell functions.

Overexpression of γ2-adaptin blocks HBV particle assembly and release by entrapping core and L in detergent-insoluble membranes. Previously, we showed that HBV formation depends on the cellular γ2-adaptin protein that independently interacts with L and core and colocalizes with both proteins in endosomal compartments (15, 37). Using small-interfering-RNA-mediated depletion of γ2-adaptin, we found that disruption of these interactions inhibits virion release without compromising envelope maturation and nucleocapsid assembly (37). Given the essential but still unclear role of γ2-adaptin in the late stages of the HBV life cycle, we reasoned that its overexpression might enhance virus production. To test this possibility, HuH-7 cells were cotransfected with an HA-tagged version of γ2-adaptin and the HBV replicon at a 3:1 DNA ratio, and cellular lysates and supernatants were probed for the formation of progeny virus particles, using the EPR assay. Contrary to our expectation, overexpression of γ2-adaptin significantly reduced the amounts of intracellular nucleocapsids and, as a consequence, the numbers of released virions (Fig. 6A, lanes 1 and 2). Viral titers were decreased 70- to 80-fold in multiple repetitions of this experiment, even though the ectopic overexpression of γ2-adaptin had no measurable effects on the overall cell viability, as indicated by the unaffected levels of cellular Hsc70 (Fig. 6A, lanes 1 and 2). As shown by South-

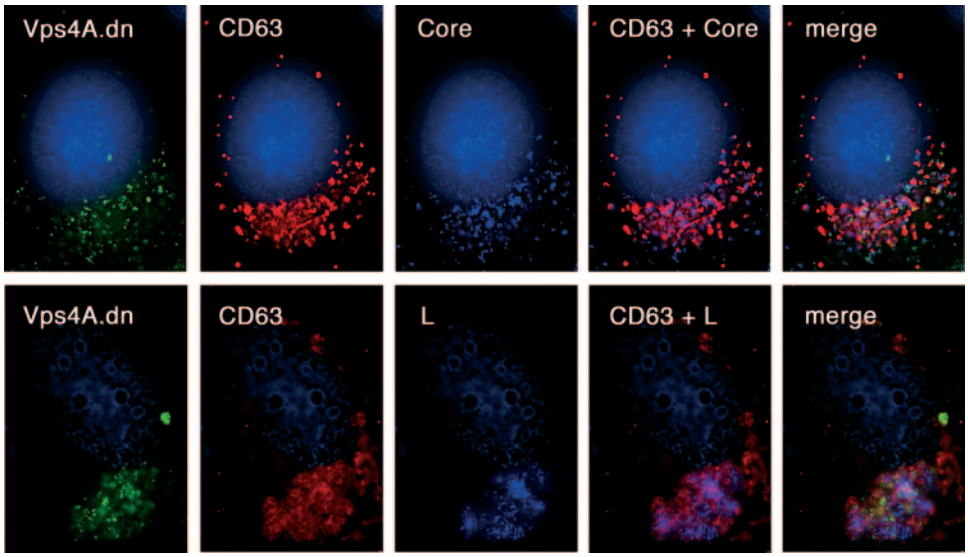

FIG. 5. HBV core and L colocalize with CD63 in dn-Vps4A-induced endosomal class E compartments. HBV-replicating cells expressing GFP-tagged Vps4A.dn were immunostained for core and CD63 (top row) or for L and CD63 (bottom row), using rabbit anti-core or rabbit anti-L antibodies, respectively, and mouse anti-CD63 antibodies. The immune complexes were detected by staining them with AlexaFluor 647-conjugated goat anti-rabbit immunoglobulin G and AlexaFluor 594-conjugated goat anti-mouse immunoglobulin G antibodies. The autofluorescent signal of dn Vps4A is shown in green, staining of CD63 is shown in red, and the staining patterns of core and L are indicated in light blue, while DNA staining of the cell nuclei is shown in dark blue. The overlays of the CD63/core and CD63/L fluorescences are shown in the fourth images from the left column, with purple indicating colocalization. Colocalization between all three proteins is indicated by white in the corresponding merged images.

ern blot analysis of total DNA extracted from transfected cells, overexpressed γ2-adaptin also had no effect on intracellular HBV genome replication (Fig. 6A, lanes 3 and 4). Because this result was strikingly similar to those obtained with the dn ESCRT-III and Vps4 mutants, we next examined protein synthesis, stability, and solubility in HBV-replicating cells overexpressing γ2-adaptin. As described above, cell lysates were prepared with buffers containing either NP-40 or SDS, and equal amounts of samples were subjected to Western blot analyses. HA-specific immunoblotting confirmed stable synthesis of γ2-adaptin and yielded a signal in the expected position of 90 kDa that was not apparent in control-transfected cells (Fig. 6A). Like the MVB inhibitors, overexpressed γ2-adaptin led to a specific down-regulation of core and L levels in the NP-40 lysate, whereas the amount of core recovered from the SDS lysate was identical to that of control cells (Fig. 6A). For L, we again observed its nonextractability even by SDS. Collectively, these data demonstrate that excess γ2-adaptin blocked HBV production by sequestering core and L to NP-40-resistant polymers, potentially class E-like compartments. Such a sequestration was also detectable when core alone was coexpressed with γ2-adaptin (Fig. 6B), indicating that it occurred even in the absence of the other viral products. Furthermore, titration experiments showed that γ2-adaptin shifted core to NP-40-resistant structures in a dose-dependent manner (Fig. 6B), a property reminiscent of the mode of action of dn ESCRT and Vps4 mutants.

TABLE 1. Insensitivity of subviral S envelope particle release to MVB inhibition

Transfection	S reactivity in ELISA[a]	
	Lysate	Medium
S + control	1.432 ± 0.056	2.121 ± 0.097
S + CHMP4C.dn	1.354 ± 0.067	2.024 ± 0.091
S + Vps4A.wt	1.469 ± 0.063	1.859 ± 0.051
S + Vps4A.dn	1.331 ± 0.036	1.623 ± 0.036
Env + control	1.419 ± 0.041	3.668 ± 0.038
Env + CHMP4C.dn	0.779 ± 0.052	1.157 ± 0.071
Env + Vps4A.wt	1.354 ± 0.071	3.612 ± 0.023
Env + Vps4A.dn	0.741 ± 0.096	1.318 ± 0.089

[a] Amounts of S were measured by ELISA and are expressed as mean units of optical density at 492 nm ± standard deviations ($n = 3$).

Overexpression of γ2-adaptin induces a class E-like compartment. To substantiate this unexpected feature of excess γ2-adaptin, we examined the effect of its overexpression on the morphology of endosomal structures by immunofluorescence studies. As outlined above, expression of dn CHMP or Vps4 mutants resulted in the development of abnormally enlarged endosomal compartments (4, 9, 26, 43). These could be visualized by staining the cells with antibodies against CD63. In nontransfected cells serving as controls, as well as in cells synthesizing wt Vps4A, anti-CD63 labeled numerous small vesicles dispersed throughout the cytoplasm (Fig. 7). By contrast, the CD63-positive structures were strongly enlarged upon expression of dn Vps4A, CHMP3, and CHMP4B with a considerable overlap and an accumulation of each mutant on these structures, as indicated by the yellow fluorescence in the merged images (Fig. 7). Intriguingly, an even more pronounced enlargement of the CD63 fluorescent signal was observed when cells transfected with the HA-tagged γ2-adaptin were costained with anti-CD63 and anti-HA antibodies. γ2-Adaptin was located throughout the cytoplasm and induced

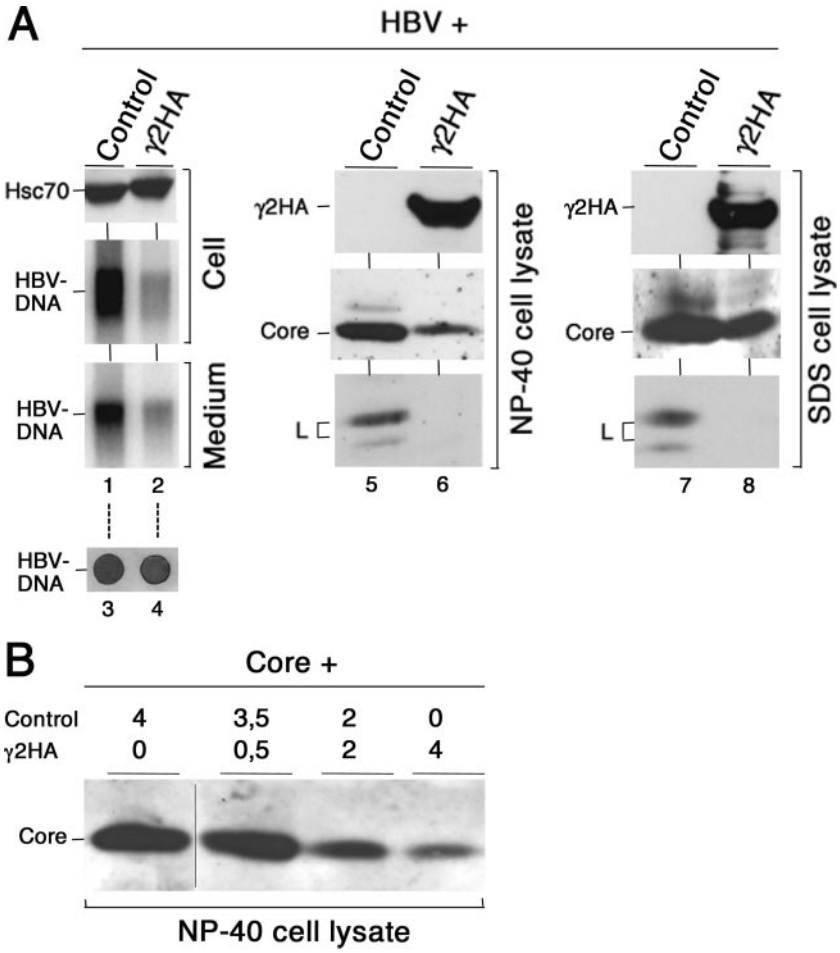

FIG. 6. Overexpressed γ2-adaptin inhibits HBV production and egress by entrapping core and L on detergent-insoluble membranes. (A) HuH-7 cells were cotransfected with the HBV replicon (HBV) and HA-tagged γ2-adaptin (γ2HA) or an empty expression vector serving as a negative control. Each cotransfection was done at a 1:3 DNA ratio, and cellular supernatants and lysates were harvested after 3 days. Virus production was monitored with the EPR assay by analyzing nucleocapsid formation within the cell and virion release in the cell medium (lanes 1 and 2), as in Fig. 2A. In a parallel experiment, transfected cells were lysed after 5 days, and total cellular DNA was harvested and analyzed by dot blot hybridization (lanes 3 and 4), as in Fig. 2B. For control of protein expression and solubility, cotransfected cells were lysed with either NP-40 or SDS, and equal amounts of extracts (25% of lysates) were analyzed by HA-, core-, L- (lanes 4 to 8), and Hsc70-specific (lanes 1 and 2) Western blotting. The positions of the corresponding proteins are indicated on the left. (B) HuH-7 cells were transfected with an expression vector carrying the HBV core gene (Core), together with increasing amounts of HA-tagged γ2-adaptin (γ2HA), as indicated above the lanes. Total DNA used for transfections was adjusted with empty-plasmid DNA (Control). Lysates were prepared using NP-40, and equal amounts of lysates (25% of lysates) were assayed by core-specific immunoblotting.

partly gigantic endosomal structures that stained positive for CD63 (Fig. 7). Together, these results indicate that γ2-adaptin, if overexpressed, shares characteristic features with dn MVB inhibitors in terms of HBV inhibition and perturbation of endosomal morphology.

Overexpression of γ2-adaptin traps MLV Gag on detergent-insoluble membranes and suppresses VLP release. To further explore the possibility that overexpressed γ2-adaptin may act as a principal inhibitor of the MVB machinery and hence of virus particle release, we analyzed the fate of a retroviral Gag protein in the presence of excess γ2-adaptin. As a reporter, we chose MLV Gag, whose budding is known to depend on a functional MVB pathway (29, 38). Because retroviral Gag proteins alone can form VLPs and exit from cells even without envelope proteins, we used an expression vector of MLV Gag full-length precursor protein in which the viral polymerase was replaced by YFP (39). It was cotransfected with HA-tagged γ2-adaptin at a 1:1 ratio in HuH-7 cells. The expression and solubility profile of cell-associated MLV Gag were assessed using the NP-40 cell lysis method as described above. In contrast, the NP-40-insoluble cell material was resolubilized with SDS lysis buffer rather than by duplicate transfections, and samples were subjected to anti-GFP (YFP)-specific Western blotting. In the absence of ectopically expressed γ2-adaptin, a specific band corresponding to MLV Gag-YFP was detected in the NP-40 lysate with only trace amounts in the corresponding SDS fraction (Fig. 8). In contrast, overexpressed γ2-adaptin shifted a large portion of MLV Gag-YFP into the NP-40-resistant SDS fraction (Fig. 8), as was the case for the HBV core protein. Moreover, when culture media of transfected cells were assessed for the release of MLV Gag-YFP, excess γ2-adaptin significantly suppressed the release of VLPs (Fig.

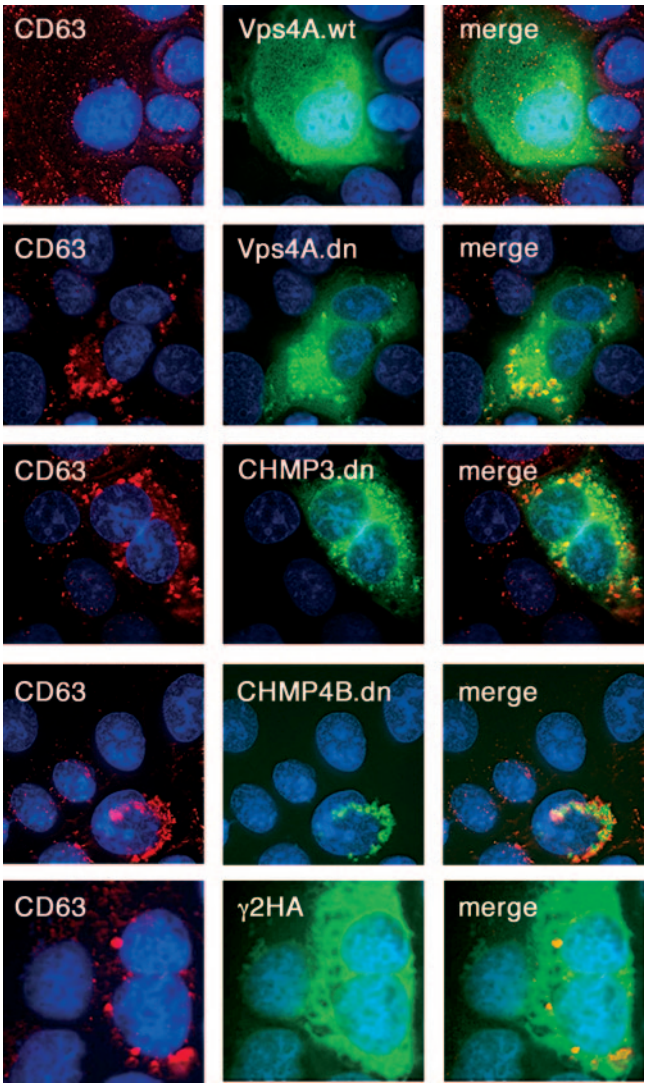

FIG. 7. Overexpressed γ2-adaptin induces endosomal class E-like compartments. HuH-7 cells were individually transfected with GFP-tagged wt or dn Vps4A, GFP-tagged dn CHMP3, DsRed-tagged dn CHMP4B, and HA-tagged γ2-adaptin (γ2HA). The cells were fixed, and γ2-adaptin-transfected cells were immunostained with mouse anti-CD63 and rat anti-HA antibodies, followed by staining with AlexaFluor 488-conjugated goat anti-mouse and AlexaFluor 546-conjugated goat anti-rat immunoglobulin G antibodies. Cells expressing the autofluorescent GFP/DsRed-tagged Vps4A and CHMP constructs were stained for CD63 alone, using AlexaFluor 546-conjugated goat anti-mouse antibodies. The fluorescent signals of wt and dn Vps4A, dn CHMP3, dn CHMP4C, and γ2-adaptin are shown in green (middle), the staining pattern of CD63 is red (left), and colocalization is shown in yellow in the merged images (right). DNA staining of the cell nuclei is shown in blue.

8). Collectively, these data imply that overexpressed γ2-adaptin behaves as a bona fide inhibitor of the MVB pathway.

DISCUSSION

This study demonstrates that HBV maturation and egress depend on late MVB pathway functions and identifies γ2-adaptin as a genuine cofactor of MVB-assisted virus budding.

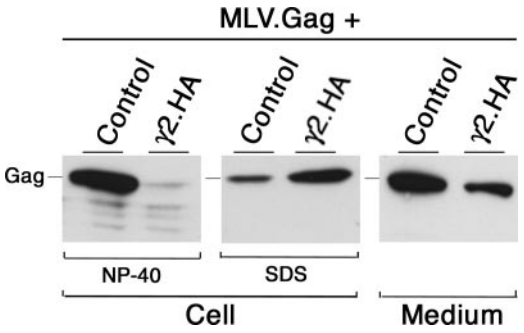

FIG. 8. Overexpressed γ2-adaptin sequesters MLV Gag to detergent-insoluble membranes and suppresses VLP release. HuH-7 cells were transfected with a plasmid encoding an MLV Gag-YFP protein (MLV.Gag), together with HA-tagged γ2-adaptin (γ2HA) or empty-plasmid DNA (Control). In contrast to the experiments shown in Fig. 3 and 6A, the cells were lysed with NP-40 (250 μl), and the NP-40-insoluble cell material was resolubilized with SDS lysis buffer (250 μl). Equal amounts of samples (60 μl) were analyzed by GFP-specific Western blotting for the detection of MLV Gag-YFP (Cell). VLPs released into the media were recovered by ultracentrifugation, and the solubilized pellets (corresponding to 25% of cellular supernatants) were analyzed as were the lysates (Medium).

Thus, HBV biogenesis shares considerable similarities with budding processes of enveloped RNA viruses, raising the possibility that different classes of virus may exit the cell by appropriating functions of the endosomal sorting machinery.

In principal, the MVB pathway is responsible for sorting cargo proteins destined for lysosomal degradation or exosomal secretion into intraluminal vesicles. Because the biogenesis of such vesicles is topologically equivalent to budding processes of membrane-containing viruses, intense research in the last few years has revealed that enveloped RNA viruses, like retroviruses, rhabdoviruses, and filoviruses, use MVB pathway functions to bud from host cells (3, 31, 35, 40). The Gag and matrix proteins of these viruses have been shown to usurp MVB sorting factors by recruitment of TSG101, Alix/AIP1, or Nedd4 by their PTAP, YPXL, or PPXY late domain, respectively. Tsg101 is the ubiquitin-interacting subunit of ESCRT-I, and there is compelling evidence that the entire heterotrimeric ESCRT-I complex functions directly in PTAP-dependent virus release (11, 13, 20). Viruses encoding YPXL late domains appear to access the MVB pathway via Alix/AIP1, which is not a permanent subunit of any of the three ESCRT complexes but likely bridges ESCRT-I and ESCRT-III (30, 38, 41). Budding of PPXY-type late-domain-containing RNA viruses primarily requires the action of the ubiquitin ligase Nedd4 (29, 38). However, thus far, it is uncertain how and where PPXY/Nedd4 complexes first meet the MVB pathway. Despite their distinct entry gates, all of these late domains of enveloped RNA viruses appear to be under the control of ESCRT-III and Vps4, which function more directly in vesicle formation (24).

Here, we showed that an enveloped DNA virus also utilizes at least the downstream MVB factors to escape the cell. Upon expression of different dn ESCRT-III mutant proteins, like CHMP3, CHMP4B, and CHMP4C, as well as ATPase-defective dn mutants of the Vps4A or Vps4B human isoforms in HBV-replicating liver cell lines, virus assembly and release were potently inhibited by each mutant. For Vps4A, our result

is consistent with a very recent communication that reported a block to HBV export imposed by Vps4A.E228Q without addressing the underlying mechanism (21). By using biochemical fractionation and immunofluorescence analyses, we observed that the ESCRT-III and Vps4 mutants prevented HBV maturation by forming enlarged endosome-derived, detergent-insoluble structures, reminiscent of class E compartments. In analogy to retroviral Gag proteins (41, 43), the HBV core became sequestered to these structures, concomitant with a block in subsequent assembly steps. In contrast to retroviruses that can bud even in the absence of the envelope, HBV requires both core and envelope structures for particle egress. Therefore, our study also focused on the S and L envelope proteins and revealed that L likewise accumulated on aberrant endosomal structures. To our knowledge, this is the first demonstration that a viral envelope can be trapped on endosomal vacuoles upon inhibition of late MVB functions. Together, these experiments establish roles for ESCRT-III and Vps4 in HBV assembly and suggest that virus particle budding takes place at the MVB.

Conversely, the assembly of subviral HBV envelope particles composed of the small S protein alone required neither the action of ESCRT-III and Vps4 (Table 1) nor the function of γ2-adaptin, as shown previously (37). Thus, the viral and subviral HBV assembly pathways seemingly differ in their requirements for cell functions and trafficking routes. One master molecule directing the route of virus assembly apart from the subviral S budding place may be γ2-adaptin, as it functionally interacts with the viral key players core and L but does not recognize S (15, 37). A trafficking role for γ2-adaptin during HBV production would be consistent with known functions of adaptor protein complex subunits that sort their specific cargo proteins to membrane compartments (5). In analogy, a recent report demonstrated that the δ-adaptin subunit of the AP-3 complex is responsible for bringing the Gag protein of human immunodeficiency virus type 1 (HIV-1) to the MVB, where Gag acquires components of the ESCRT pathway that are essential for HIV-1 budding (8).

Because depletion of γ2-adaptin inhibits HBV release (37), here, we studied the consequences of its overexpression for virus production and observed a similar inhibitory effect. Together, these results confirm the critical role of γ2-adaptin in HBV budding and, furthermore, indicate that virus particle formation is very sensitive to alterations in γ2-adaptin expression. The most likely interpretation of the overexpression experiments is that excess of full-length γ2-adaptin acts in a dn fashion on its endogenous orthologue. Accordingly, overexpressed γ2-adaptin may interfere with HBV formation by perturbing the correct stoichiometry of the interaction between γ2-adaptin, core, and L, or other proteins required for this process. Similar observations have been made for other cellular factors assisting in late steps of retrovirus production. For instance, the budding of equine infectious anemia virus depends on Alix/AIP1 and can be blocked by both overexpression and small interfering RNA silencing of this endocytic factor (7). In the case of HIV-1, Tsg101 controls the assembly of VLPs, and its up- and down-regulation critically interfere with this process (11, 13). An imbalance in the concentration of binding partners may thus interfere with productive interactions required for viral export.

It is important to recognize that alternative mechanisms can be proposed to explain the inhibitory effect of excess γ2-adaptin on HBV production. In particular, we noted that overexpressed γ2-adaptin shifted core and L to detergent-insoluble membrane structures, a hallmark accompanying aberrant endosome induction (26) that is not observed in γ2-adaptin-depleted cells (37). It is therefore equally conceivable that excess γ2-adaptin blocks HBV production indirectly by inducing dysfunctional endosomal compartments in a manner similar to dn ESCRT-III or Vps4 mutants. Indeed, we could show that up-regulated γ2-adaptin perturbed normal endosomal morphology and sequestered the retroviral MLV Gag, a known substrate of the MVB machinery (38), to detergent-insoluble structures, along with a decrease in VLP release. These data suggest that γ2-adaptin, if present in excess, can act as a general dominant inhibitor of the MVB pathway and, conversely, may normally operate within this pathway. This proposal requires direct testing in further experiments. A complementary clue for this proposal is our recent finding that γ2-adaptin is unique among the classic adaptor protein subunits in its ubiquitin-binding activity (37), a feature shared by a number of ESCRT components (40).

These findings and previous reports demonstrating that productive HBV particle formation utilizes γ2-adaptin together with MVB pathway functions (21, 37) have potential implications for virus particle assembly. It is not yet known where core and the envelope first meet within the cell. Because excess γ2-adaptin and dn ESCRT-III and Vps4 mutants can trap core in detergent-insoluble structures even in the absence of the viral envelope (Fig. 5 and our unpublished observations), a direct core-L interaction is unlikely to initiate the recruitment of core to membranes. In favor of this, the core particle of the related duck HBV has been shown to associate with membranes in an envelope-independent manner (28). One possibility is that membrane targeting of core may be enabled by Nedd4, which binds to its late-domain-like PPAY motif (37). The Nedd4-core complex would next be recognized by γ2-adaptin, either directly or in conjunction with ubiquitin, thereby providing a link to the MVB cascade. In this respect, it is tempting to speculate that γ2-adaptin may present one of the yet-uncharacterized adaptors involved in bridging Nedd4-substrate complexes to the MVB machinery. The HBV envelope proteins that exit the ER and enter the Golgi compartment (23) may gain access to the MVB pathway via the physical association of L with γ2-adaptin. In this scenario, HBV virions would then bud into these or related compartments by utilizing ESCRT-III and Vps4 functions and exit the cell by the exosome pathway, as is the case for HIV-1 in infected macrophages and human T-lymphoblastic cell lines (14, 34). The precise mechanistic understanding of the viral release process remains to be deciphered and is a focus of ongoing investigation. In particular, future electron microscopy studies should help to unravel the structure of HBV particles arrested in budding. The finding that excess γ2-adaptin acts as a bona fide MVB inhibitor is another aspect that deserves further study.

ACKNOWLEDGMENTS

We thank E. Gottwein, K.-H. Heermann, W. Mothes, K. Nakayama, H. Schaller, C. Sureau, and W. Sundquist for generously providing plasmid DNA constructs and antibodies. We also thank K. Jaschinski

and M. Rost for critical reading of the manuscript and helpful discussions.

This work was supported by grants to R.P. from the Deutsche Forschungsgemeinschaft (SFB 490-D1 and PR 305/1-3).

REFERENCES

1. **Babst, M., D. J. Katzmann, E. J. Estepa-Sabal, T. Meerloo, and S. D. Emr.** 2002. Escrt-III: an endosome-associated heterooligomeric protein complex required for mvb sorting. Dev. Cell **3:**271–282.
2. **Babst, M., D. J. Katzmann, W. B. Snyder, B. Wendland, and S. D. Emr.** 2002. Endosome-associated complex, ESCRT-II, recruits transport machinery for protein sorting at the multivesicular body. Dev. Cell **3:**283–289.
3. **Bieniasz, P. D.** 2006. Late budding domains and host proteins in enveloped virus release. Virology **344:**55–63.
4. **Bishop, N., and P. Woodman.** 2000. ATPase-defective mammalian VPS4 localizes to aberrant endosomes and impairs cholesterol trafficking. Mol. Biol. Cell **11:**227–239.
5. **Boehm, M., and J. S. Bonifacino.** 2001. Adaptins: the final recount. Mol. Biol. Cell **12:**2907–2920.
6. **Bruss, V.** 2007. Hepatitis B virus morphogenesis. World J. Gastroenterol. **13:**65–73.
7. **Chen, C., O. Vincent, J. Jin, O. A. Weisz, and R. C. Montelaro.** 2005. Functions of early (AP-2) and late (AIP1/ALIX) endocytic proteins in equine infectious anemia virus budding. J. Biol. Chem. **280:**40474–40480.
8. **Dong, X., H. Li, A. Derdowski, L. Ding, A. Burnett, X. Chen, T. R. Peters, T. S. Dermody, E. Woodruff, J. J. Wang, and P. Spearman.** 2005. AP-3 directs the intracellular trafficking of HIV-1 Gag and plays a key role in particle assembly. Cell **120:**663–674.
9. **Fujita, H., M. Yamanaka, K. Imamura, Y. Tanaka, A. Nara, T. Yoshimori, S. Yokota, and M. Himeno.** 2003. A dominant negative form of the AAA ATPase SKD1/VPS4 impairs membrane trafficking out of endosomal/lysosomal compartments: class E *vps* phenotype in mammalian cells. J. Cell Sci. **116:**401–414.
10. **Ganem, D., and A. M. Prince.** 2004. Hepatitis B virus infection—natural history and clinical consequences. N. Engl. J. Med. **350:**1118–1129.
11. **Garrus, J. E., U. K. von Schwedler, O. W. Pornillos, S. G. Morham, K. H. Zavitz, H. E. Wang, D. A. Wettstein, K. M. Stray, M. Cote, R. L. Rich, D. G. Myszka, and W. I. Sundquist.** 2001. Tsg101 and the vacuolar protein sorting pathway are essential for HIV-1 budding. Cell **107:**55–65.
12. **Glebe, D., and S. Urban.** 2007. Viral and cellular determinants involved in hepadnaviral entry. World J. Gastroenterol. **13:**22–38.
13. **Goff, A., L. S. Ehrlich, S. N. Cohen, and C. A. Carter.** 2003. Tsg101 control of human immunodeficiency virus type 1 Gag trafficking and release. J. Virol. **77:**9173–9182.
14. **Grigorov, B., F. Arcanger, P. Roingeard, J. L. Darlix, and D. Muriaux.** 2006. Assembly of infectious HIV-1 in human epithelial and T-lymphoblastic cell lines. J. Mol. Biol. **359:**848–862.
15. **Hartmann-Stuhler, C., and R. Prange.** 2001. Hepatitis B virus large envelope protein interacts with gamma2-adaptin, a clathrin adaptor-related protein. J. Virol. **75:**5343–5351.
16. **Heermann, K. H., U. Goldmann, W. Schwartz, T. Seyffarth, H. Baumgarten, and W. H. Gerlich.** 1984. Large surface proteins of hepatitis B virus containing the pre-S sequence. J. Virol. **52:**396–402.
17. **Huovila, A. P., A. M. Eder, and S. D. Fuller.** 1992. Hepatitis B surface antigen assembles in a post-ER, pre-Golgi compartment. J. Cell Biol. **118:**1305–1320.
18. **Ingham, R. J., G. Gish, and T. Pawson.** 2004. The Nedd4 family of E3 ubiquitin ligases: functional diversity within a common modular architecture. Oncogene **23:**1972–1984.
19. **Jaoude, G. A., and C. Sureau.** 2005. Role of the antigenic loop of the hepatitis B virus envelope proteins in infectivity of hepatitis delta virus. J. Virol. **79:**10460–10466.
20. **Katzmann, D. J., M. Babst, and S. D. Emr.** 2001. Ubiquitin-dependent sorting into the multivesicular body pathway requires the function of a conserved endosomal protein sorting complex, ESCRT-I. Cell **106:**145–155.
21. **Kian Chua, P., M. H. Lin, and C. Shih.** 2006. Potent inhibition of human hepatitis B virus replication by a host factor Vps4. Virology **354:**1–6.
22. **Kobayashi, T., M. H. Beuchat, J. Chevallier, A. Makino, N. Mayran, J. M. Escola, C. Lebrand, P. Cosson, and J. Gruenberg.** 2002. Separation and characterization of late endosomal membrane domains. J. Biol. Chem. **277:**32157–32164.
23. **Lambert, C., and R. Prange.** 2001. Dual topology of the hepatitis B virus large envelope protein: determinants influencing post-translational pre-S translocation. J. Biol. Chem. **276:**22265–22272.
24. **Langelier, C., U. K. von Schwedler, R. D. Fisher, I. De Domenico, P. L. White, C. P. Hill, J. Kaplan, D. Ward, and W. I. Sundquist.** 2006. Human ESCRT-II complex and its role in human immunodeficiency virus type 1 release. J. Virol. **80:**9465–9480.
25. **Lewin, D. A., D. Sheff, C. E. Ooi, J. A. Whitney, E. Yamamoto, L. M. Chicione, P. Webster, J. S. Bonifacino, and I. Mellman.** 1998. Cloning, expression, and localization of a novel gamma-adaptin-like molecule. FEBS Lett. **435:**263–268.
26. **Lin, Y., L. A. Kimpler, T. V. Naismith, J. M. Lauer, and P. I. Hanson.** 2005. Interaction of the mammalian endosomal sorting complex required for transport (ESCRT) III protein hSnf7-1 with itself, membranes, and the AAA+ ATPase SKD1. J. Biol. Chem. **280:**12799–12809.
27. **Loffler-Mary, H., J. Dumortier, C. Klentsch-Zimmer, and R. Prange.** 2000. Hepatitis B virus assembly is sensitive to changes in the cytosolic S loop of the envelope proteins. Virology **270:**358–367.
28. **Mabit, H., and H. Schaller.** 2000. Intracellular hepadnavirus nucleocapsids are selected for secretion by envelope protein-independent membrane binding. J. Virol. **74:**11472–11478.
29. **Martin-Serrano, J., S. W. Eastman, W. Chung, and P. D. Bieniasz.** 2005. HECT ubiquitin ligases link viral and cellular PPXY motifs to the vacuolar protein-sorting pathway. J. Cell Biol. **168:**89–101.
30. **Martin-Serrano, J., A. Yarovoy, D. Perez-Caballero, and P. D. Bieniasz.** 2003. Divergent retroviral late-budding domains recruit vacuolar protein sorting factors by using alternative adaptor proteins. Proc. Natl. Acad. Sci. USA **100:**12414–12419.
31. **Morita, E., and W. I. Sundquist.** 2004. Retrovirus budding. Annu. Rev. Cell Dev. Biol. **20:**395–425.
32. **Nassal, M.** 1999. Hepatitis B virus replication: novel roles for virus-host interactions. Intervirology **42:**100–116.
33. **Patient, R., C. Hourioux, P. Y. Sizaret, S. Trassard, C. Sureau, and P. Roingeard.** 2007. Hepatitis B subviral envelope particle morphogenesis and intracellular trafficking. J. Virol. **81:**3842–3851.
34. **Pelchen-Matthews, A., B. Kramer, and M. Marsh.** 2003. Infectious HIV-1 assembles in late endosomes in primary macrophages. J. Cell Biol. **162:**443–455.
35. **Pelchen-Matthews, A., G. Raposo, and M. Marsh.** 2004. Endosomes, exosomes and Trojan viruses. Trends Microbiol. **12:**310–316.
36. **Radziwill, G., W. Tucker, and H. Schaller.** 1990. Mutational analysis of the hepatitis B virus P gene product: domain structure and RNase H activity. J. Virol. **64:**613–620.
37. **Rost, M., S. Mann, C. Lambert, T. Doring, N. Thome, and R. Prange.** 2006. Gamma-adaptin, a novel ubiquitin-interacting adaptor, and Nedd4 ubiquitin ligase control hepatitis B virus maturation. J. Biol. Chem. **281:**29297–29308.
38. **Segura-Morales, C., C. Pescia, C. Chatellard-Causse, R. Sadoul, E. Bertrand, and E. Basyuk.** 2005. Tsg101 and Alix interact with murine leukemia virus Gag and cooperate with Nedd4 ubiquitin ligases during budding. J. Biol. Chem. **280:**27004–27012.
39. **Sherer, N. M., M. J. Lehmann, L. F. Jimenez-Soto, A. Ingmundson, S. M. Horner, G. Cicchetti, P. G. Allen, M. Pypaert, J. M. Cunningham, and W. Mothes.** 2003. Visualization of retroviral replication in living cells reveals budding into multivesicular bodies. Traffic **4:**785–801.
40. **Slagsvold, T., K. Pattni, L. Malerod, and H. Stenmark.** 2006. Endosomal and non-endosomal functions of ESCRT proteins. Trends Cell Biol. **16:**317–326.
41. **Strack, B., A. Calistri, S. Craig, E. Popova, and H. G. Gottlinger.** 2003. AIP1/ALIX is a binding partner for HIV-1 p6 and EIAV p9 functioning in virus budding. Cell **114:**689–699.
42. **Takatsu, H., M. Sakurai, H. W. Shin, K. Murakami, and K. Nakayama.** 1998. Identification and characterization of novel clathrin adaptor-related proteins. J. Biol. Chem. **273:**24693–24700.
43. **von Schwedler, U. K., M. Stuchell, B. Muller, D. M. Ward, H. Y. Chung, E. Morita, H. E. Wang, T. Davis, G. P. He, D. M. Cimbora, A. Scott, H. G. Krausslich, J. Kaplan, S. G. Morham, and W. I. Sundquist.** 2003. The protein network of HIV budding. Cell **114:**701–713.
44. **Yorikawa, C., H. Shibata, S. Waguri, K. Hatta, M. Horii, K. Katoh, T. Kobayashi, Y. Uchiyama, and M. Maki.** 2005. Human CHMP6, a myristoylated ESCRT-III protein, interacts directly with an ESCRT-II component EAP20 and regulates endosomal cargo sorting. Biochem. J. **387:**17–26.
45. **Zizioli, D., C. Meyer, G. Guhde, P. Saftig, K. von Figura, and P. Schu.** 1999. Early embryonic death of mice deficient in gamma-adaptin. J. Biol. Chem. **274:**5385–5390.